Title: Aggregation of an RNA-binding protein, not loss of heterochromatin, causes sterility of aging yeast cells

Authors: Gavin Schlissel†[1], Marek K. Krzyzanowski†[2], Fabrice Caudron[2,3], Yves Barral[2], Jasper Rine*[1]

Affiliations:

† - These authors contributed equally to this work.

1 - Department of Molecular and Cell Biology, UC Berkeley.

2 - Institute of Biochemistry, ETH Zurich.

3 - King's College London.

*Correspondence to: jrine@berkeley.edu

Abstract:

In yeast, heterochromatin silencing is reported to decline in aging mother cells causing sterility in old cells. This process is thought to reflect a decrease in the activity of the NAD^+-dependent deacetylase Sir2. Here, we tested whether Sir2 becomes nonfunctional gradually or precipitously during aging. Unexpectedly, silencing of the heterochromatic *HML* and *HMR* loci was not lost during aging. Old cells could initiate a mating response, however they were less sensitive to mating pheromone than were young cells due to age-dependent aggregation of Whi3, an RNA-binding protein controlling S-phase entry. Removing the poly-glutamine domain of Whi3 restored the pheromone sensitivity of old cells. We propose that aging phenotypes previously attributed to loss of heterochromatin silencing are instead caused by aggregation of the Whi3 cell-cycle regulator.

One sentence summary: Old cells lose sensitivity to α-factor, but that phenotype wasn't caused by failure of Sir2: it was caused by aggregation of the G1/S inhibitor Whi3.

Main text:

Budding yeast divide asymmetrically, and each yeast mother cell produces a finite number of daughter cells in her lifetime. This process—yeast replicative aging—has been studied for insights into aging more broadly because the processes that underlie aging in yeast might be related to factors that underlie aging in other asymmetrically dividing cells (*1*).

In *Saccharomyces cerevisiae*, haploid mother cells lose the ability to mate as they age (*2*). It was proposed that old mother cells fail to mate as a consequence of a decline of Sir2 function, which would cause loss of heterochromatic gene silencing of the auxiliary mating type loci *HML* and *HMR* (*3*). Loss of silencing at *HML* and *HMR* in old cells has been attributed to the redistribution of Sir proteins to the nucleolus and to a decrease in available Sir2 (*4–6*). Furthermore, old cells may either be either limited for the Sir2 substrate NAD+ or may be exposed to high concentrations of nicotinamide (NAM), an inhibitor of Sir2, resulting in the inactivation of Sir2 in old cells and thus sterility (*7–9*).

We characterized transcriptional repression by Sir2 by testing whether transient loss-of-silencing events at *HML* might precede the complete loss of silencing attributed to the oldest cells. To study silencing at *HML* in a yeast mother cell, we monitored pedigrees of haploid cells carrying a Cre-based silencing reporter (*10*). The reporter uses a Cre recombinase gene inserted in place of *HMLα2*, and a fluorescent reporter inserted at a euchromatic locus elsewhere in the genome (Fig. 1A). Loss of silencing at *hmlα2Δ::CRE* induces a permanent and heritable switch from expressing red fluorescent protein to expressing green fluorescent protein (Fig. 1A), and the

sensitivity of the Cre reporter approaches the sensitivity of single molecule RNA florescent *in situ* hybridization (*10*). We manually separated daughter cells from their mothers to analyze pedigrees in two common strain backgrounds, S288c and W303, and observed no loss-of-silencing events in dozens of pedigrees of haploids, diploids and hybrids (Fig. 1B).

To measure the frequency of silencing loss as a function of a cell's lifespan, we extended the pedigree analysis by using a microfluidic device that traps mother cells and separates their buds. We analyzed more than 1500 yeast pedigrees at single cell resolution and observed 13 loss-of-silencing events (Fig. 1C, movie S1). Furthermore, we found that a cell's age did not affect its ability to maintain silencing of *HML*, and the overwhelming majority of yeast mother cells stopped dividing without even a transient loss of silencing (Fig. 1D). As a control, when Sir2 activity in old cells was inhibited by addition of nicotinamide, all surviving cells lost silencing suggesting that old cells did not accumulate nicotinamide in amounts that inactivate Sir2 (Fig. 1E, movie S2). Similar results were obtained by analyzing a green fluorescent protein gene inserted in place of *HMLα* and with an alternative microfluidic design, indicating that the observation was independent of the reporter and the microfluidic setup used (Fig. S1). Previous studies have shown that Sir2 protein levels decrease in cells older than seven generations old, however we found no evidence of a decrease in Sir2 activity at *HML* (*4*). It is possible that a decrease in Sir2 levels in old cells could affect other Sir2 complexes, including the nucleolar RENT complex. Inactivating the RENT complex would decrease rDNA silencing and increase the occurrence of extrachromosomal rDNA circles in old cells, two phenotypes that have been repeatedly observed in old cells (1).

We also purified populations of aged *MATα* cells from liquid culture and analyzed them for expression of RNA from the *HMR* locus. Old cells cultured for ~20 generations showed low

expression of *HMRa1* mRNA relative to cells cultured in the presence of the Sir2 inhibitor nicotinamide, establishing that Sir2-dependent silencing of auxiliary mating type loci was functional in old cells (Fig. 2A,B). In addition to analyzing silenced RNA from *HMR,* we analyzed expression of *STE3*, which encodes the a-factor pheromone receptor, is expressed in *MAT*α cells and is repressed in diploids. *STE3* expression did not reflect a repressed diploid-like gene expression program that would be expected if mating-type information from *HMR* were expressed (Fig. 2A,B).

Although the *HML* and *HMR* loci are the premier context for studying Sir-based transcriptional repression, published RNA sequencing of cells lacking Sir2 has identified the full complement of genes that are subject to repression by Sir2 (*13*). Separately RNA sequencing data has been published from matched young and old cells, which includes RNA expression data from these Sir2-regulated loci (*14*). We reanalyzed these data to ascertain whether Sir2-regulated genes show age-associated changes in transcription that could reflect loss of Sir2 function. Genome-wide, we found no evidence that Sir2-dependent gene regulation was related to aging-dependent gene regulation (Fig. 2C). Furthermore, telomeric open reading frames repressed directly by Sir2 showed no evidence of an age-dependent increase in transcription (Fig. S2). In short, we found no evidence that the transcriptional program in *sir2*Δ cells was similar to the transcriptional program in old yeast cells.

Having shown that *HML* and *HMR* were silenced during aging, we reinvestigated the sterility phenotype reported for old cells (*3*, *12*). We treated young and old *MATa* cells with various amounts of α-factor pheromone and monitored their ability to arrest in G1 and grow a mating projection (Fig 3A). Previous experiments that identified an age-associated mating defect used assays sensitized by using a low concentration (less than 20ng/mL) of α-factor (3). Indeed,

we found that old mother cells (mean age: 14.3 divisions) responded less efficiently to mating pheromone than did young cells; however, they responded efficiently with pheromone concentrations above 20 ng/mL (Fig. 3B). If the observed loss of mating depended on expression from *HML,* then deletion of *HML* would restore the sensitivity of old cells to the level of young cells, which was not the case (Fig. 3C). Young and old yeast deleted for *HMLα2* were more responsive to α-factor than were wild type cells (Fig. 3C and Fig. S3). Arrest with α-factor did not affect the stability of silencing at *HML,* indicating that the heightened sensitivity in *hmlα2*Δ mutants did not reflect transcription from *HML* during α-factor treatment (Fig. S4).

Efficient response to mating pheromone depends on arrest in the G1 phase of the cell cycle. Cells exposed to α-factor for longer than four hours escape this cell cycle arrest and become less sensitive to pheromone (*15*). This adaptation depends on aggregation and subsequent inactivation of Whi3, an RNA-binding S-phase inhibitor, but desensitized mothers produce daughters that are fully sensitive to α-factor (*15*). Old cells showed a similar asymmetric inheritance of mating competence: the daughters of old cells were more responsive to α-factor than were their mothers (Fig. 4A). To test whether aggregation of Whi3 might explain why old yeast mother cells fail to respond to α-factor, we deleted a glutamine-rich domain required for Whi3 aggregation in cells adapted to α-factor and assayed old *MATa* cells carrying this deletion for α-factor responsiveness. Indeed, deletion of the Whi3 glutamine-rich domain decreased the loss of sensitivity in old cells, indicating that Whi3 aggregation may prevent mating in old cells (Fig. 4B). Live-cell imaging of old yeast mother cells expressing a green florescent protein-tagged Whi3 indicated that old yeast cells did form aggregates of Whi3 (Fig. 4C,D and Fig. S5). Interestingly, *whi3-*Δ*polyQ* strains lived slightly longer than wild-type strains, suggesting that aggregation of Whi3 might limit lifespan (Fig. 4E).

Although our conclusions regarding whether aging impacts gene silencing stand in contrast with previous work, the methods we used were more sensitive and extensive than those available in the past. Although it would be best to repeat analyses with exactly the same strains used previously, over the years those strains have been lost, precluding a direct comparison. Nevertheless, our data establish that age-dependent loss of gene silencing is not a feature of widely used budding yeast strains.

The mechanism by which yeast deleted for *HML* show slightly decreased sensitivity to mating pheromone independent of transcription at the locus is unclear. Interruption of the silent *HML* locus could have an indirect effect on mating factor sensitivity, perhaps by inducing changes in the three-dimensional architecture of chromosome III that affect expression of genes involved in the α-factor response.

Both yeast and vertebrates are rich in RNA-binding proteins containing low-complexity prion-like domains. Unlike aggregates of typical yeast prions, Whi3 aggregates are sequestered in the mother cell during cell division (*15*). Aggregation during aging may be an intrinsic liability for yeast memory factors (mnemons) like Whi3 that encode memory in the form of protein aggregates. In this view, aging-induced aggregation of Whi3 would preclude alpha-factor induced Whi3 aggregation as a memory of past unsuccessful mating encounters. It is tempting to speculate that in nature yeast could benefit from a *bona-fide* differentiation between old and young cells, with some aggregates being beneficial and others not. Understanding why Whi3 aggregates form and are retained in the mother cell during mitosis may shed light on how protein aggregation influences the mitotic inheritance of cytoplasmic factors more broadly.

References and Notes:

1. L. Guarente, C. Kenyon, Genetic pathways that regulate ageing in model organisms. *Nature*. **408**, 255–262 (2000).

2. I. Müller, Parental age and the life-span of zygotes of Saccharomyces cerevisiae. *Antonie Van Leeuwenhoek*. **51**, 1–10 (1985).

3. T. Smeal, J. Claus, B. Kennedy, F. Cole, L. Guarente, Loss of transcriptional silencing causes sterility in old mother cells of S. cerevisiae. *Cell*. **84**, 633–642 (1996).

4. D. L. Lindstrom, C. K. Leverich, K. A. Henderson, D. E. Gottschling, Replicative age induces mitotic recombination in the ribosomal RNA gene cluster of Saccharomyces cerevisiae. *PLoS Genet.* **7**, e1002015 (2011).

5. W. Dang, K. K. Steffen, R. Perry, J. A. Dorsey, Histone H4 lysine 16 acetylation regulates cellular lifespan. *Nature* (2009).

6. B. K. Kennedy *et al.*, Redistribution of silencing proteins from telomeres to the nucleolus is associated with extension of life span in S. cerevisiae. *Cell*. **89**, 381–391 (1997).

7. S. J. Lin, P. a Defossez, L. Guarente, Requirement of NAD and SIR2 for life-span extension by calorie restriction in Saccharomyces cerevisiae. *Science*. **289**, 2126–2128 (2000).

8. G. R. F. & L. G. Su-Ju Lin*, Matt Kaeberlein*†, Alex A. Andalis‡, Lori A. Sturtz§, Pierre-Antoine Defossez*†, Valeria C. Culotta§, Calorie restriction extends Saccharomyces cerevisiae lifespan by increasing respiration. *Nature*. **418**, 336–40 (2002).

9. R. M. Anderson, K. J. Bitterman, J. G. Wood, O. Medvedik, D. A. Sinclair, Nicotinamide and PNC1 govern lifespan extension by calorie restriction in Saccharomyces cerevisiae. *Nature*. **423**, 181–5 (2003).

10. A. E. Dodson, J. Rine, Heritable capture of heterochromatin dynamics in Saccharomyces

cerevisiae. *Elife*. **4**, e05007 (2015).

11. M. C. Jo, W. Liu, L. Gu, W. Dang, L. Qin, High-throughput analysis of yeast replicative aging using a microfluidic system. *Proc. Natl. Acad. Sci.*, 201510328 (2015).

12. K. Ashrafi, D. Sinclair, J. I. Gordon, L. Guarente, Passage through stationary phase advances replicative aging in Saccharomyces cerevisiae. *Proc. Natl. Acad. Sci. U. S. A.* **96**, 9100–9105 (1999).

13. A. Ellahi, D. M. Thurtle, J. Rine, The Chromatin and Transcriptional Landscape of Native Saccharomyces cerevisiae Telomeres and Subtelomeric Domains. *Genetics*. **200**, 505–521 (2015).

14. P. Sen *et al.*, H3K36 methylation promotes longevity by enhancing transcriptional fidelity. *Genes Dev.* **29**, 1362–1376 (2015).

15. F. Caudron, Y. Barral, A Super-Assembly of Whi3 encodes memory of deceptive encounters by single cells during yeast courtship. *Cell*. **155**, 1244–1257 (2013).

16. S.S. Lee, I.A. Vizcarra, D. Huberts, L. Lee, M Heineman. Whole lifespan microscopic observation of budding yeast aging through a microfluidic dissection platform. *PNAS* (2012), vol. 109, pp. 4916–4920.

17. D. H. E. W. Huberts *et al.*, Construction and use of a microfluidic dissection platform for long-term imaging of cellular processes in budding yeast. *Nat. Protoc.* **8**, 1019–27 (2013).

18. A. L. Hughes, C. E. Hughes, K. A. Henderson, N. Yazvenko, D. E. Gottschling, Selective sorting and destruction of mitochondrial membrane proteins in aged yeast. *Elife*. **5**, e13943 (2016).

19. D. M. Thurtle-Schmidt, A. E. Dodson, J. Rine, Histone Deacetylases with Antagonistic Roles in Saccharomyces cerevisiae Heterochromatin Formation. *Genetics* (2016).

20. H. Wickham, Elegant Graphics for Data Analysis. *Media*. **35**, 211 (2009).

21. R Developement Core Team, R: A Language and Environment for Statistical Computing. *R Found. Stat. Comput.* **1**, 409 (2015).

22. B. K. Kennedy, N.R. Austriaco Jr, Guarente L. Daughter cells of Saccharomyces cerevisiae from old mothers display a reduced life span. *J Cell Biol*, **127**, 1985-1993 (1994)

Acknowledgements: We thank M. Delarue, N. Azgui and the UC Berkeley biotechnology nanofabrication facility for assistance in fabricating microfluidic devices, and E. Unal and G. Brar for microscopy support. We thank S. Guetg for providing the *hml::GFP* reporter, S.S. Lee for advice on microfluidics, light microscopy center of ETH Zurich (ScopeM), T. Schwarz for technical support, and T. Kruitwagen for critical reading of the manuscript. RNA sequencing data from Ellahi et al (14) is available from NCBI accession numbers SRX884375, SRX885291, SRX885292, SRX885297, SRX885304, SRX885305 and RNA sequencing data from Sen et al (15) is at NCBI as series GSE65767. This work was supported by a grant from the National Institutes of Health (GM31105, GS and JR), and by the ETH Zürich and European Research Council BarrAge (FC and YB), and by an iPHD fellowship from SystemsX.ch (MK).

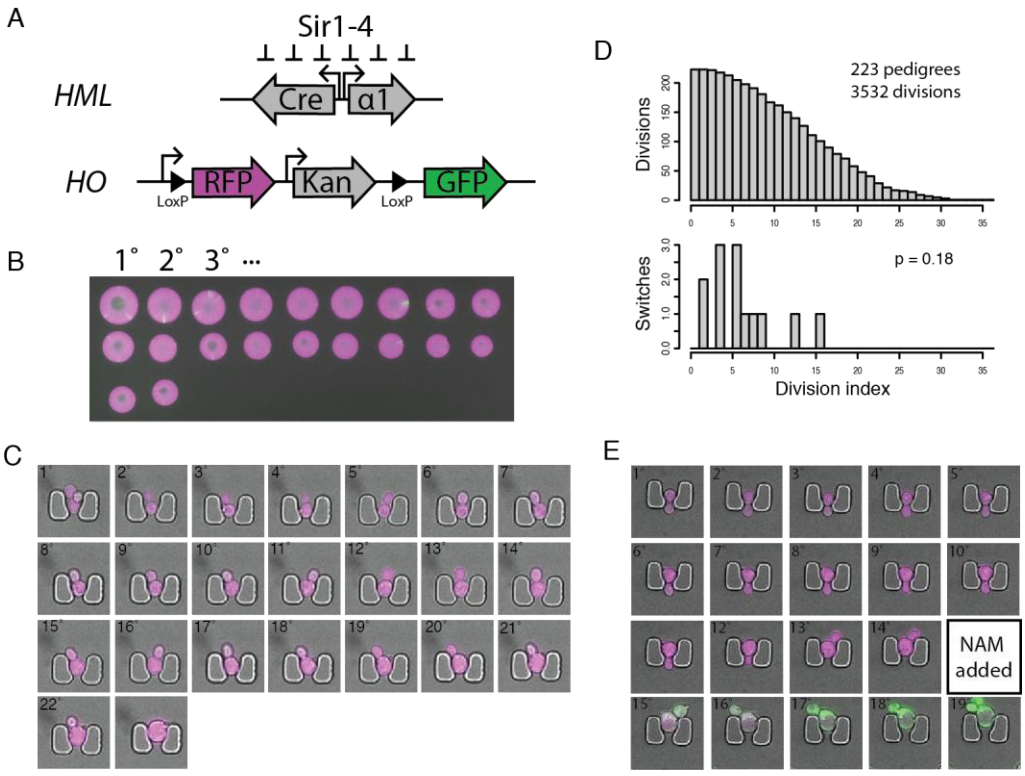

Fig 1. Loss of silencing is not a feature of yeast aging.

(**A**) Schematic of the CRASH (**C**re-**R**eported **A**ltered **S**tates of **H**eterochromatin) reporter (*10*). (**B**) Representative pedigree of 20 sequential daughters from W303 haploid strain (JRY10774) carrying the CRASH reporter. (**C**) Frames depict each division event in a typical pedigree in the S288C haploid strain background (JRY10772). (**D**) Top - histogram of all cell-division events that occurred for 223 pedigrees from a microfluidic experiment using JRY10772. Bottom - the age of cells at the time they lost silencing is plotted as a histogram for the 13 pedigrees that lost silencing. Division index refers to the number of buds that each mother produced after the cells were loaded on the microfluidic chip, and the p-value was calculated using the Kolmogorov-Smirnov test. (**E**) Frames depict consecutive daughters of a pedigree as in (C), and nicotinamide (NAM) was added to the medium after ~24h.

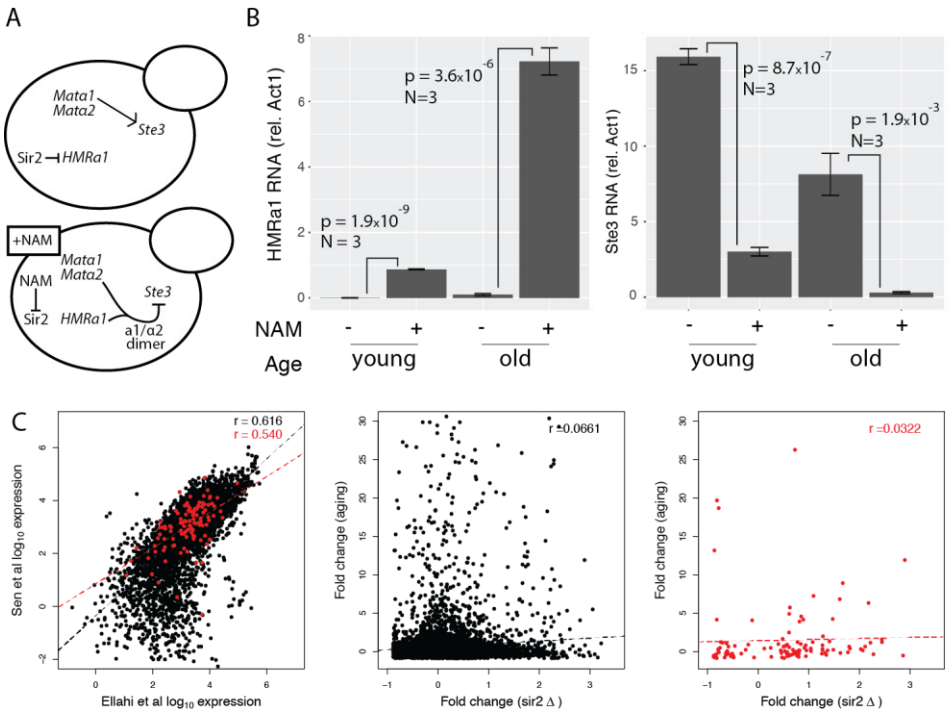

Fig 2. Mating pathways genes did not show diploid-like RNA expression in old cells.

(**A**) Schematic of mating-factor receptor regulation for a *MATα* haploid strain. (**B**) RT-qPCR for the Sir2-regulated *HMRa1* RNA and the mating-type regulated *STE3* mRNA. To account for difficulty in handling small numbers of cells (10^6-10^7 old cells were prepared for RT-qPCR), we restricted our analysis to direct comparison of age-matched samples where the RNA preparation conditions were directly comparable. P-values were calculated by two-tailed T-test. (**C**) Reanalysis of published RNA sequencing data. At left, young cells from two different publications (*13*, *14*) showed repeatable RNA expression. Red dots indicate genes that are regulated by Sir2 as defined by Ellahi *et al* (*13*). At center, fold-change in expression is plotted for old cells from Sen *et al* (*14*) compared to matched young cells and for *sir2*Δ cells from Ellahi *et al* (*13*) compared to a matched wild-type control strain. At right, the subset of genes from the center panel that were identified as Sir regulated by Ellahi *et al* are plotted.

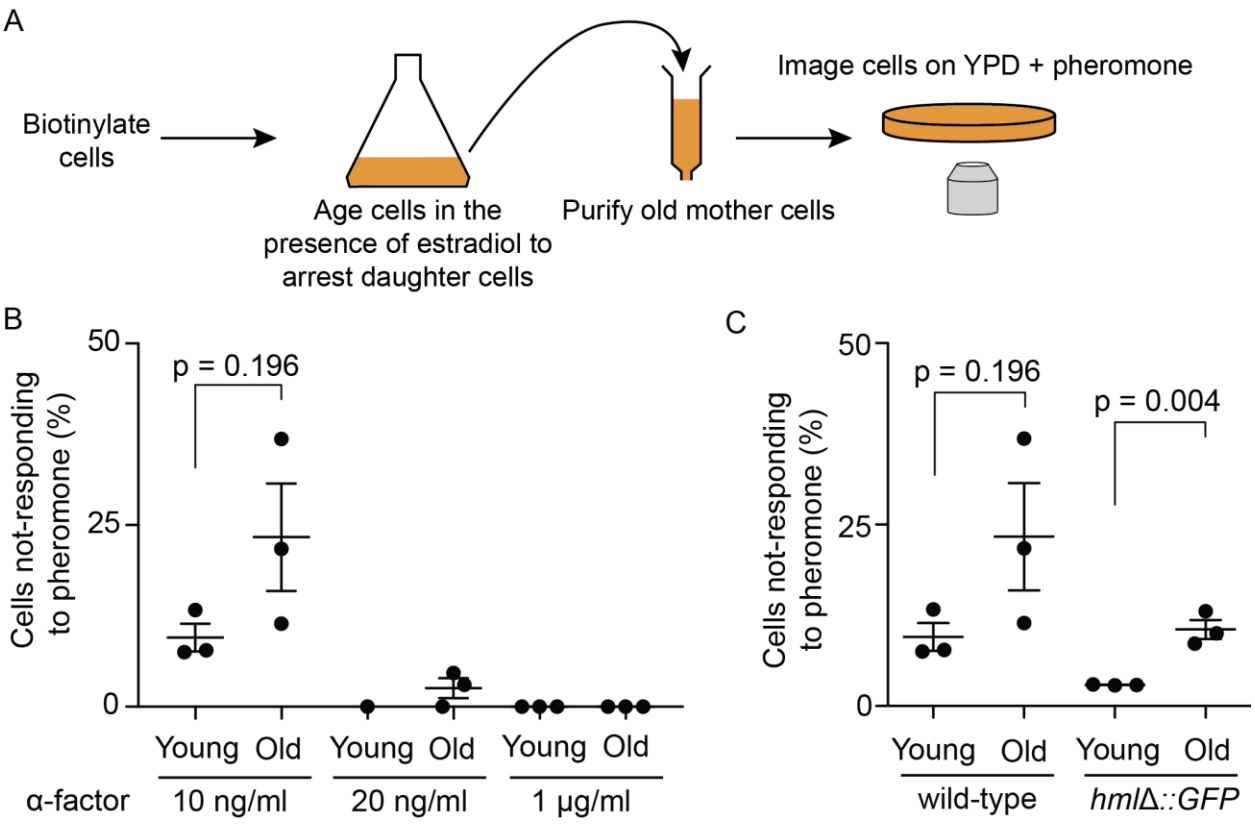

Fig 3. Old cells required a higher pheromone dose than young cells to form a mating projection. (**A**) Schematic of the experimental approach (**B**) Young and old (on average 14 divisions old) *MATa* cells (yYB4172) were purified from 2 hour and 20 hour cultures, respectively, and their response to pheromone was assayed on agar pads containing indicated α-factor concentrations. Fraction of cells not-responding to α-factor (at 10 ng/ml) increased with age, however all cells responded to higher concentrations of α-factor. (**C**) Young and old cells of yYB6829 (*hml*Δ*)* strain were tested for pheromone response to α-factor (10 ng/ml). Both wild type and *hml*Δ mutant cells lost pheromone sensitivity to a similar extent with age, however *hml*Δ cells were more sensitive to pheromone than the corresponding wild-type cells (yYB4172, data from Fig. 3B repeated for comparison. All the plots show mean values ± SEM, dots represent independent experiments (n≥30 cells). P values were calculated by two-tailed T-test.

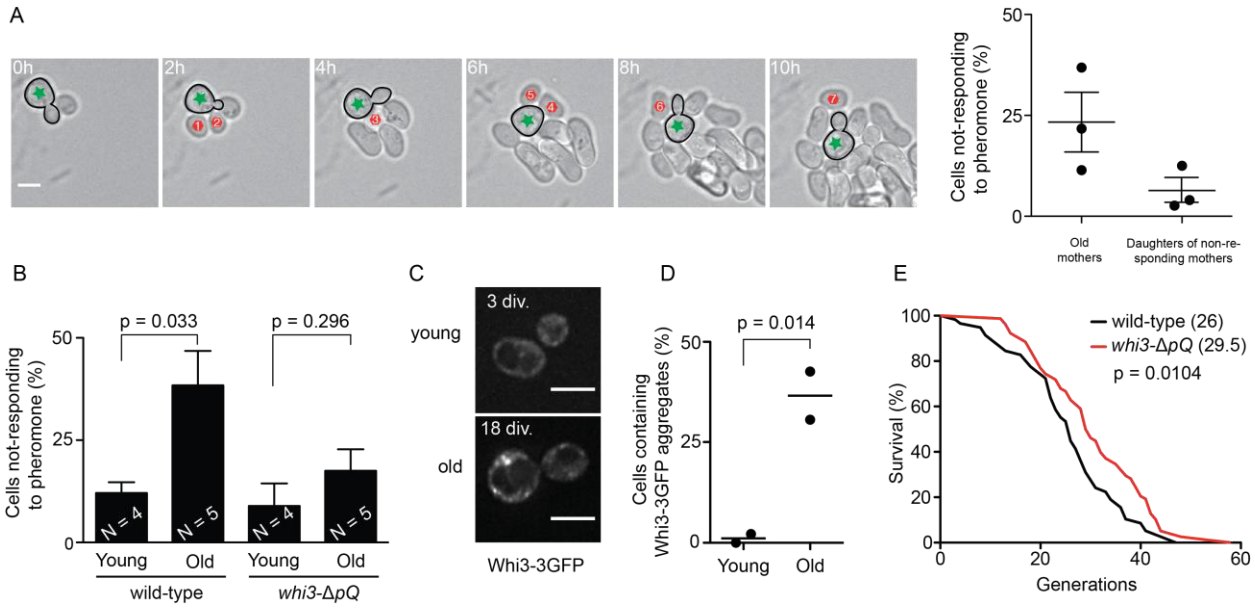

Fig 4. Formation of Whi3 aggregates contributes to the loss of pheromone sensitivity with age. (**A**) Left: example sequence showing old mother cell and her progeny exposed to α-factor (10 ng/ml). An old mother cell (green asterisk) buds instead of responding to pheromone, but her daughters arrest in G1 and form mating projections. Right: quantification of pheromone response of first 3 daughters of pheromone-insensitive old mothers of yYB4172 from figure 3B. (**B**) Old and young *MATa* cells were exposed to α-factor (10 ng/ml). Pheromone insensitivity increased with age in the wild-type strain (3.2-fold between young and old cells) while this effect was reduced in *whi3-ΔpQ* cells (1.9-fold increase). Young cells were ~5 divisions old, and old cells were between 15 and 20 divisions old. Bars show mean value ± SEM (young cells total n > 200, old cells total n > 170). P-values were calculated by unpaired two-tailed T-test. (**C**) Whi3 forms aggregates in old cells. (**D**) Quantification of the fraction of cells containing Whi3-3GFP aggregates in young and aged yeast cells. Each dot represents an independent experiment and p-value indicates one-tailed T-test. **(E)** Survival curves of wild-type and whi3-ΔpQ strains (wild type yYB14326 n = 58, whi3-ΔpQ yYB14325 n = 78 cells). Deletion of the glutamine-rich domain of Whi3 extends lifespan. P-value was calculated with the Log-rank (Mantel-Cox) test.

Supplementary Materials:

Materials and methods

Supplementary figures S1-S5

Supplementary movies S1-S2

Supplementary table S1

Supplementary Materials for

Aggregation of an RNA-binding protein, not loss of heterochromatin, causes sterility of aging yeast cells

Gavin Schlissel†, Marek K. Krzyzanowski†, Fabrice Caudron, Yves Barral, Jasper Rine*
† - equal contribution
*correspondence to: jrine@berkeley.edu

This PDF file includes:

Other Suplementary Materials for this manuscript includes the following:

Materials and Methods

Media and growth conditions

All strains used in this study are described in table S1. For pedigree analysis, cells were grown 24 hours in filtered YPD (2% dextrose) and diluted as necessary to ensure cultures did not reach stationary phase. Microfluidic experiments used YPD (2% dextrose) with Ampicillin (50µg/uL) and nicotinamide (NAM, 5mM) as required for the experiment. For RNA analysis, founder cells were kept in exponential phase for 24 hours in YPD (2% dextrose). After biotinylation, cells were diluted into 1L of YPD (2% dextrose) with 1µM estradiol and 50µg/mL ampicillin with 5mM nicotinamide as required for the experiment.

Microfluidic dissection of yeast pedigrees

Two different microfluidic devices were used. For experiments using the Cre-Lox silencing reporter, microfluidic chips were fabricated as described previously with minor modifications (*11*). A negative chrome mask was ordered (Front Range Photo Mask), and used to fabricate the negative mold. Here, we built the mold on 100mm mechanical grade silicon wafers (University Wafer) using SU-8 2005 (MicroChem) instead of SU-8 3005. The SU-8 negative mold had a feature height of 5.0 µM. Microfluidic devices were cast in PDMS (Sylgard) and cut such that each device contained only a single working media inlet and outlet and a single cell inlet per device. The PDMS devices were bonded to 24x60mm #1 thickness cover slips (Fisher). For experiments using the GFP reporter at *HML*, the microfluidic chip was prepared as described previously using a negative master mold obtained from the authors (*16*, *17*).

Operation of microfluidic dissection platform

The microfluidic device and accessory tubing were purged with filtered media at a flow rate of 20µL per minute using a syringe pump driving 30 or 60 mL plastic syringes (BD Falcon). When the chip was purged, the cell inlet tube was attached to the single working cell inlet port, and manually injected cells at a concentration of 10^5-10^6 cells per mL. Restricting cells to the intended lane of the microfluidic device was problematic, so backflow from the cell inlet was allowed to seed all channels of the chip. After the device was seeded, media was supplied at a rate of 7µL per minute for to up to 72 hours. For experiments in which the growth medium was changed, a second syringe pump was connected to the media inlet port with a wye junction and Tygon tubing. The second syringe pump was purged and pressurized with the rest of the microfluidic device, and the switch between media sources was performed by manually adjusting the flow rate on each pump. Cells were held at 30°C in an incubation chamber attached to the stage of a Deltavision microscope (Olympus), and were imaged every 10 minutes with a 60x objective for RFP, GFP and DIC channels. Data were processed and visualized with ImageJ software and pedigrees were analyzed manually. To measure the *hml::GFP* using the microfluidic device designed by Lee et al (*16*), the device was primed with synthetic complete medium (SC, 2% dextrose), and cells were loaded manually as described previously (*16*). Cells trapped under the PDMS pads were flushed constantly with 1 µL/min flow of SC medium supplied from 10 ml syringe pump. The microfluidic device was mounted on an Eclipse Ti epifluorescent microscope (Nikon Instruments), equipped with Orca R2 CCD camera (Hamamatsu) and 60x/1.4NA Plan Apo objective, and incubation chamber set at 30°C. Budding events were monitored by capturing images every 20 minutes for 42 hours using Micro Manager 1.4 software. GFP signal was captured in old and young cells obtained in the device by capturing

stacks of seven, 1 µm thick, slices every 40 minutes for 4 h 40 min, using a mercury lamp (Intensilight, Nikon Instruments). After capturing the first GFP time point (untreated cells), the flow was switched manually to SC media + 5 mM NAM, first at a rate of 10 µL/min for 1h (to ensure complete replacement of the chamber and tubing volume with new medium), followed by 4 h at 2 µL/min, as a positive control for reporter activity. Most cells started expressing GFP signal within 2 hours after switching the media source. Total amount of the GFP signal for single cells was measured in sum projections using ImageJ software and plotted against their age.

Enrichment of old cells for RNA analysis

Old cells were enriched as published previously with minor modifications (*18*). For RNA experiments, old cells were purified using 30µL Dynabeads MyOne C1 magnetic beads (Invitrogen) per sample in 2mL microcentrifuge tubes using a standard magnetic stand separator.

Assaying pheromone responsiveness of old cells

Old cells were obtained as described previously, with modifications (*18*). Briefly, prior to experiments cells were kept in exponential growth for >14 hours, washed with PBS and labeled with EZ-Link Sulfo-NHS-LC-Biotin (Pierce). Total of 1.8 x 10^7 of biotinylated cells were inoculated in 500 ml YPD medium containing 1 µM estradiol and 50 µg/mL ampicillin and cultured at 30°C for 18-20 hours to obtain old cells, and 2 hours for young cells. Cells were purified using 65 µL of streptavidin-coated magnetic beads, LS MACS columns (Miltenyi Biotec) and quadro-MACS separator (Miltenyi Biotec). Cells were washed and eluted with YPD, pelleted at 650 x g at room temperature and split in half. One half was fixed for age determination and second half placed on α-factor containing YPD agar pads placed in Lab-Tek II chambers (Thermo Fisher). Agar pads were cut out from plates prepared the previous day containing the indicated α-factor (Sigma Aldrich) concentrations and supplemented with 20 µ g/mL casein. Pheromone response of the cells was assayed by capturing transmitted light images every 10-15 min for 8 hours, using Nikon Eclipse Ti or Deltavision microscopes equipped with 60x objectives. Cells were counted as responding if they formed a mating projection within 2 cell cycles since encountering the pheromone, as quantified previously (*3*). The second half of the cells was used for age determination. Cells were fixed with 4% paraformaldehyde/3.4% sucrose solution for 15 min, pelleted and stored in KPO_4/1.2 M sorbitol solution. Budscars were stained with calcofluor white (5 µg/mL) or with tetramethylrhodamine-coupled wheat germ agglutinin (TRITC-WGA, Molecular Probes), washed with KPO_4/1.2 M sorbitol and imaged with respective filters using Nikon Eclipse Ti and Deltavision microscopes.

Quantification of Whi3-3GFP aggregates

Cells were prepared by using the mother-enrichment program as described above, after culturing for 18-24 hours for old cells or 2 hours for young cells. For live staining of bud scars, TRITC-WGA (Molecular Probes) was added to the eluted cells before pelleting, and excess dye removed with 2 washes of SC media. Cells were placed on SC agar pads and GFP and bud scars were visualized with a Deltavision microscope equipped with CCD HQ camera (Roper), using 100x objective, solid-state light-emitting diodes illumination and appropriate filters. Z-stacks of images covering the whole diameter of the cell were acquired and deconvolved using Softworx program. Cells were quantified as containing aggregates if they displayed a mass of fluorescence that was typically spanning 2-3 focal planes (≥ 1 µm) and visually distinguishable from the rest of the cytoplasm.

RNA purification and RT-qPCR

RT-qPCR was performed as described previously (*19*). Primers targeting the *HMRa1* mRNA were: oGS329 TGGATGATATTTGTAGTATGGCGGA and OGS330 TCCCTTTGGGCTCTTCTCTT. Primers targeting the *STE3* mRNA were: oGS327 GACCATGACAGGTGTGAACAAGCTA and oGS328 TGTAGATGCGGCAATATGGAGTGAC. Expression levels were normalized to *ACT1* mRNA, which was measured using primers oGS323 TGTCCTTGTACTCTTCCGGT oGS324 CCGGCCAAATCGATTCTCAA. Data were processed and visualized using R and ggplot2 (*20, 21*).

Computational re-analysis of RNA sequencing data

Data were obtained in BEDgraph format from NCBI (GSE65767) or from the authors directly (*13,14*). For aging RNA analysis, samples GSM1604370, GSM1604372 were reflect young cells, and samples GSM1604371, GSM1604373 reflect old cells. Each replicate and each strand of each data set was normalized to the same-sample genome-wide median expression value. For figure S2, data were smoothed by use of a sliding-window mean with a range of 51. The plotted value reflects the maximum expression value for each strand, where the source data were stranded. Features for the SacCer2 reference genome were obtained from the Saccharomyces Genome Database (yeastgenome.org). For differential expression analysis, raw depth-of-coverage counts were used, summing over each ORF (on the coding strand only, where stranded data were used). Data were analyzed and plotted using R software. Code is available on request.

Lifespan analysis

Pedigree analysis was performed by micromanipulation using Zeiss Axioscope microscope (Zeiss) with methods described previously (*22*). Briefly, freshly streaked cells were restreaked on YPD plates (2% dextrose) and after one division virgin daughters were picked as a starting population. During dissection cells were kept at 30°C and overnight cells were kept at 4°C (ca. 12 h). Lifespan curves were plotted and analyzed using Prism software (GraphPad).

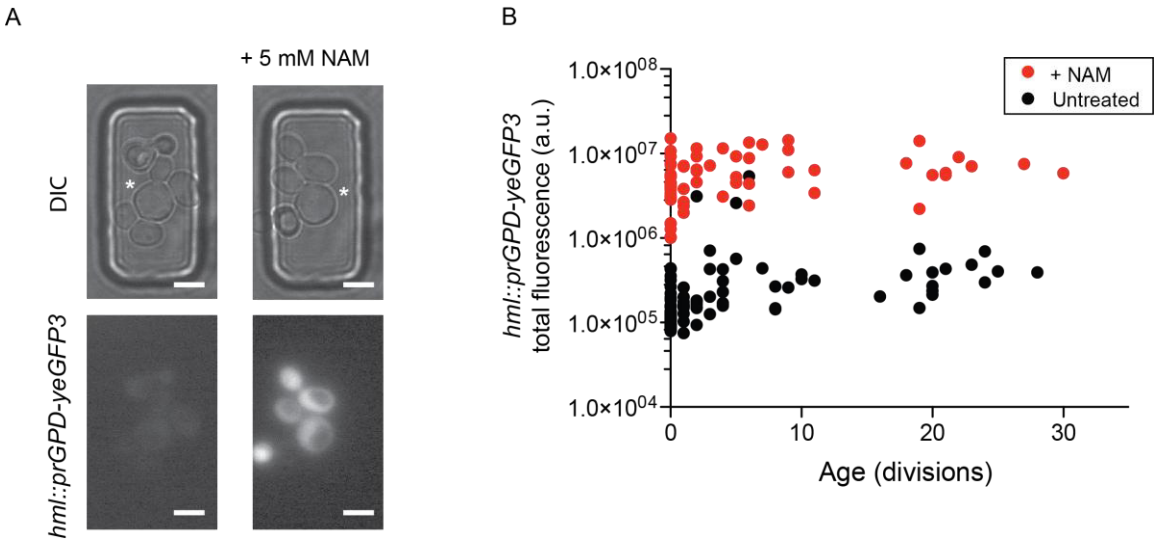

Fig. S1

Silencing of *HML* was not lost with age as assayed by a GFP reporter inserted into the locus. (**A**) Example sum projections of *hml::GFP* cells showing that in both young and old (asterisk) cells the GFP signal was low in comparison with the same cells treated with 5 mM NAM. Cells were kept in the microfluidic device for ~42 hours, allowing some of the original cells to age. The resulting cohort of old and young cells was measured for expression of the GFP reporter (left panel), next the same cohort was flushed with NAM containing media for 4 h 40 minutes (right panel). The scale bars represent 5µm. (**B**) Quantification of the GFP expression in untreated and NAM-treated cells of different age. Only few untreated young cells showed GFP expression comparable to the derepressed state, and there was no increase of the signal with age (n = 81 untreated cells, n = 66 treated).

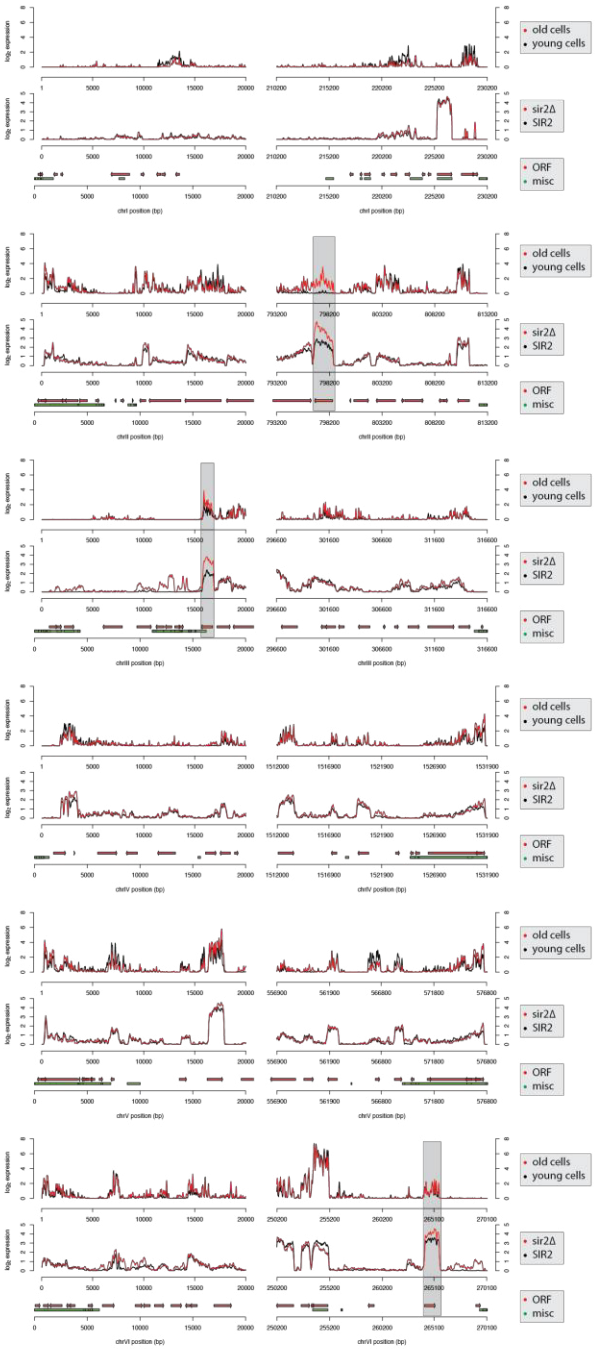
log2 expression
old cells
young cells
sir2Δ
SIR2
ORF
misc
chrI position (bp)
chrIII position (bp)
chrV position (bp)
chrVI position (bp)

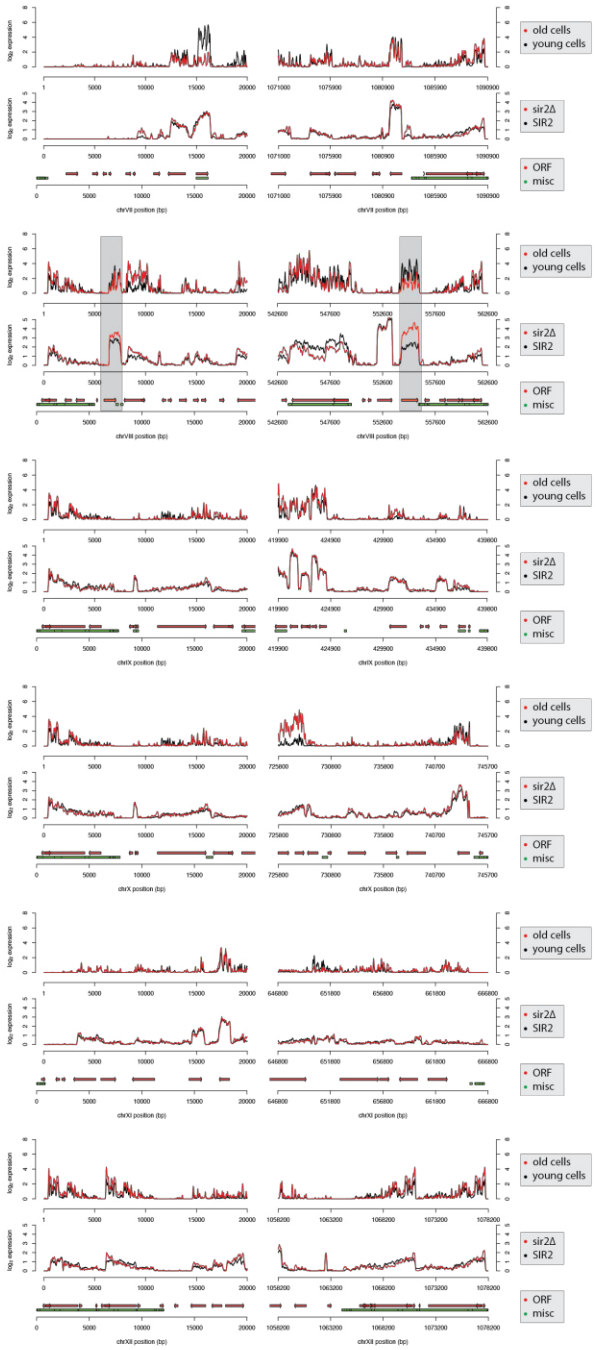
log2 expression
old cells
young cells
sir2Δ
SIR2
ORF
misc
chrVII position (bp)
chrVIII position (bp)
chrIX position (bp)
chrX position (bp)
chrXI position (bp)
chrXII position (bp)

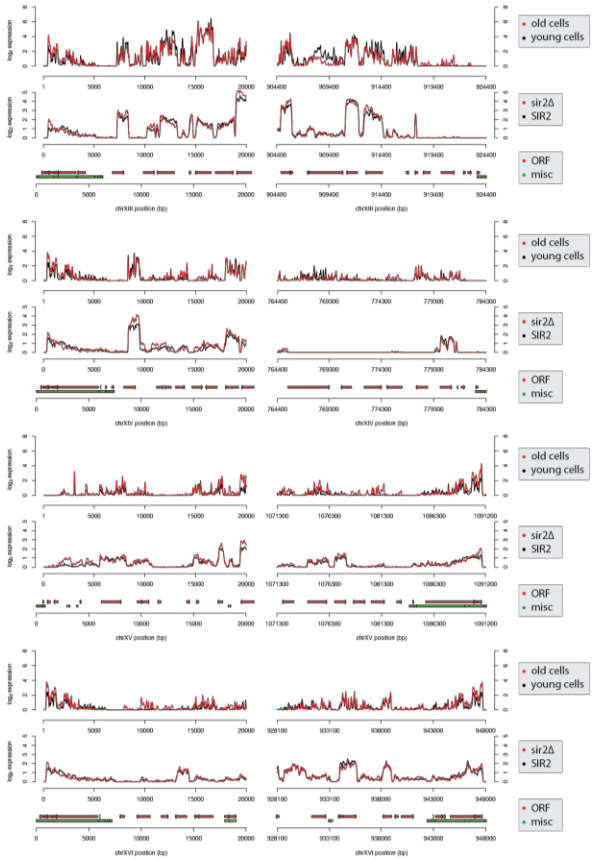

Fig. S2

Subtelomeric targets of Sir2 repression were not coherently regulated during aging. Left and right telomeres from each of the 16 chromosomes are plotted. For each chromosome, the top panel reflects data from Sen *et al* (14), where the red line corresponds to RNA from old cells and the black line corresponds to RNA from young cells. The bottom panel reflects data from Ellahi *et al* (13), where the red line corresponds to mRNA from *sir2*Δ and the black line corresponds to mRNA from *SIR2* cells. Genes identified in Ellahi *et al* as direct targets of Sir-complex repression are indicated by gray boxes. There is no correspondence between Sir2-depedent gene regulation and aging-dependent gene regulation at the telomeres.

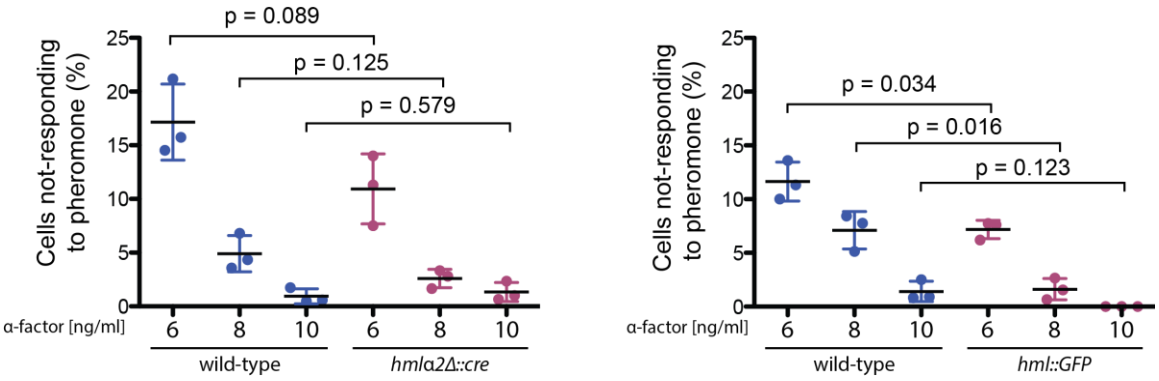

Fig. S3

MATa strains lacking the *HML* are more sensitive to pheromone. Pheromone response of the strains lacking, either both *α* genes (*hml::GFP*, yYB6829) or only *α2* (*hmlα2Δ::CRE*, yYB13584), was assayed on YPD agar pads containing 6-, 8- or 10 ng/ml α-factor. Both mutant strains were more sensitive to pheromone than the corresponding wild-type strains. P values were calcualted with two-tailed T-test.

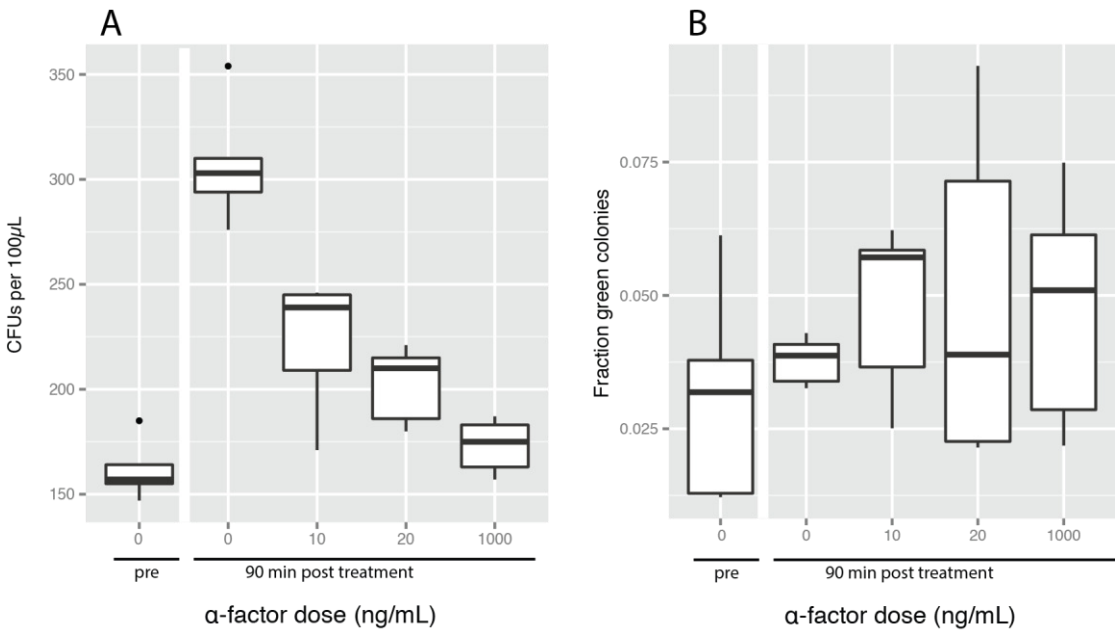

Fig. S4

α-factor treatment did not cause expression from *HML*. To test whether treatment with α-factor might disrupt silencing at *HMLα2* in a way that would make *hml*Δ strains appear more sensitive to α-factor than their wild-type counterparts, we treated log-phase *MATa* cells with the CRASH reporter at *HML* with varying concentrations of α-factor and plated to determine the fraction of cells that lose silencing when exposed to α-factor. (**A)** Total colony counts (CFUs per 100uL) show that cells arrest in a range of α-factor concentrations to varying degrees. (**B**) The fraction of colonies that are completely green-- reflecting loss of silencing before the colony formed-- is plotted across a range of α-factor exposure conditions. Under the model that α-factor treatment causes loss of silencing at *HML*, the fraction of colonies that are completely green would be expected to increase with the concentration of α-factor. We found no evidence for such an effect, suggesting that α-factor treatment does not induce transcription from *HML*.

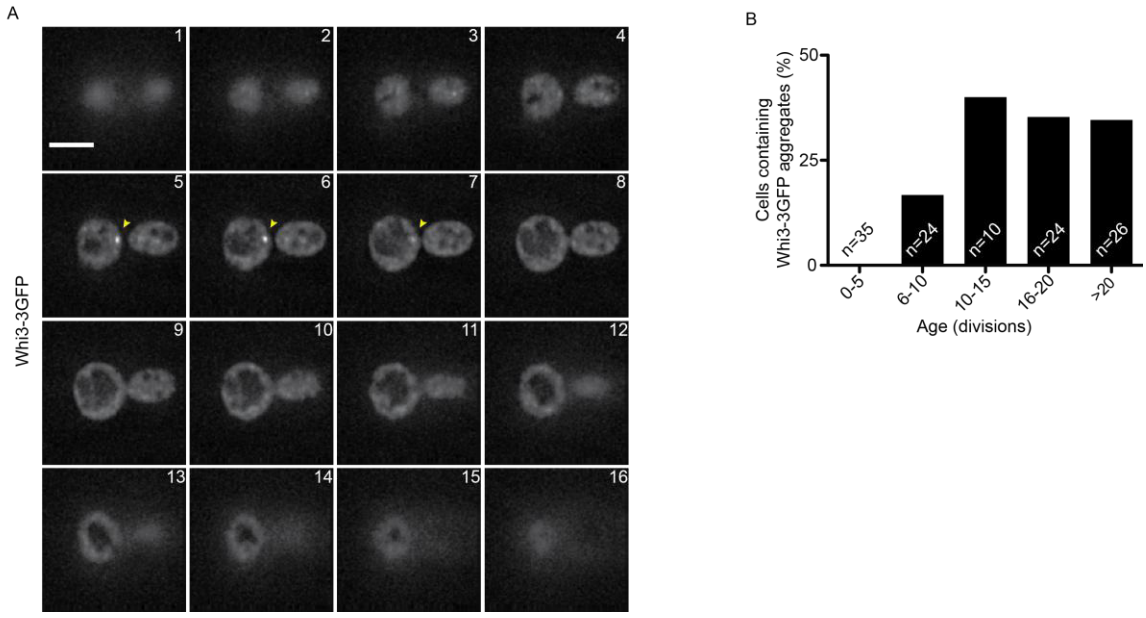

Fig. S5

Quantification of Whi3 aggregates. (**A**) Example Z-section through an old cell containing Whi3-3GFP aggregate. Typically the aggregates represented a distinct mass of intensity higher than the surrounding cytoplasm and spanning through 2-3 focal planes of 0.5 µm. The scale bar represents 5 µm. (**B**) Cells from all young (2h) and old (18-24 h) samples obtained were pooled and grouped by age categories.

Table S1.

Strains used in the present study

Strain name	Parent strain	Genotype
JRy10771	UCC5181	*MATα ade2::hisG his3 leu2 trp1Δ63 ura3Δ0 met15Δ::ADE2 hoΔ::P_{scw11}-cre-EBD78-NATMX loxp-UBC9-loxP-LEU2 loxp-CDC20-Intron-loxP-HPHMX*
JRy10772	BY4741	*MATa his3Δ1 leu2Δ0 met15Δ0 hml@2Δ::CRE hoΔ::pGPD-loxP- yEmRFP -tCYC1-KANMX-loxP-GFP-tADH1*
JRy10773	BY4742	*MATα his3Δ1 leu2Δ0 lys2Δ0 , hmlα2Δ::CRE, hoΔ::pGPD-loxP-yEmRFP-tCYC1:HYGMX:loxP-yEGFP-tADH1*
JRy10774	W303	*MATa ADE2, lys2, TRP1, hmlα2Δ::CRE, ura3Δ::pGPD-loxP-yEmRFP-tCYC1:HYGMX:loxP-yEGFP-tADH1*
JRy10775	W303	*MATα ADE2, lys2, TRP1, hmlα2Δ::CRE, ura3Δ::pGPD-loxP-yEmRFP-tCYC1:HYGMX:loxP-yEGFP-tADH1*
yYB4172	S288c	*MATa ade2::hisG his3 leu2 met15Δ::ADE2 trp1Δ63 ura3Δ0 hoΔ::SCW11pr-Cre-EBD78-NatMX loxP-UBC9-loxP-LEU2 loxP-CDC20-Intron-loxP-HPHMX bar1Δ::KanMX*
yYB6829	S288c	*MATa ade2::hisG his3 leu2 lys2 trp1Δ63 ura3Δ0 met15Δ ::ADE2 hoΔ::SCW11pr-Cre-EBD78-NatMX loxP-CDC20-Intron-loxP-HPHMX loxP-UBC9-loxP-LEU2 HML::HMLE-GPDpr-yeGFP3-HMLI-URA3 bar1Δ ::HIS3MX*
yYB6830	S288c	*MATa ade2::hisG his3 leu2 met15Δ::ADE2 ura3Δ0 trp1 hoΔ::SCW11pr-Cre-EBD78-NatMX loxP-UBC9-loxP-LEU2 loxP-CDC20-Intron-loxP-HPHMX bar1Δ::HIS3 WHI3-3GFP:kanMX*
yYB12887	S288c	*MATa ade2::hisG his3 leu2 met15Δ::ADE2 ura3Δ0 TRP1 hoΔ::SCW11pr-Cre-EBD78-NatMX loxP-UBC9-loxP-LEU2 loxP-CDC20-Intron-loxP-HPHMX bar1Δ::KanMX*
yYB12886,	S288c	*MATa ade2::hisG his3 leu2 met15D::ADE2 ura3Δ0 TRP1 hoD::SCW11pr-Cre-EBD78-NatMX loxP-UBC9-loxP-LEU2 loxP-CDC20-Intron-loxP-HPHMX bar1Δ::KanMX whi3-Q:3HA*
yYB13583	S288c	*MATa his3Δ1 leu2Δ0 met15Δ0 ura3Δ0 bar1Δ::URA3*
yYB13584	S288c	*MATa his3Δ1 leu2Δ0 met15Δ0 hmlα2Δ::CRE ura3Δ ::pGPD-loxP- yEmRFP -tCYC1-KANMX-loxP-GFP-tADH1 bar1Δ::URA3*
yYB14325		*MATa his3Δ1 leu2Δ0 ura3Δ0 whi3-Q:3HA*
yYB14326		*MATa his3Δ1 leu2Δ0 ura3Δ0*

Movie S1

Microfluidic dissection of yeast pedigrees in the S288C background using the CRASH reporter allows longitudinal analysis of a cell's silencing state.

Movie S2

Microfluidic dissection of yeast pedigrees in the S288C background using the CRASH reporter allows longitudinal analysis of a cell's silencing state. Here, the Sir2 inhibitor nicotinamide was added to the media after ~24 hours to test whether the ongoing activity of Sir2 was required for the ongoing repression of the Cre gene at *HML*.